HHS Public Access

Author manuscript

Nat Chem Biol. Author manuscript; available in PMC 2016 March 01.

Published in final edited form as:

Nat Chem Biol. 2015 September ; 11(9): 713–720. doi:10.1038/nchembio.1869.

Tunable and reversible drug control of protein production via a self-excising degron

Hokyung K. Chung[1], **Conor L. Jacobs**[1], **Yunwen Huo**[2], **Jin Yang**[3], **Stefanie A. Krumm**[4], **Richard K. Plemper**[4,5], **Roger Y. Tsien**[3,6,7], and **Michael Z. Lin**[2,8]

[1]Department of Biology, Stanford University, Stanford, CA 94305, USA

[2]Department of Pediatrics, Stanford University, Stanford, CA 94305, USA

[3]Department of Pharmacology, University of California, San Diego, La Jolla, CA 92093, USA

[4]Department of Pediatrics, Emory University, Atlanta, GA 30322, USA

[5]Institute for Biomedical Sciences, Georgia State University, Atlanta, GA 30303, USA

[6]Department of Chemistry and Biochemistry, University of California, San Diego, La Jolla, CA 92093, USA

[7]Howard Hughes Medical Institute, University of California, San Diego, La Jolla, CA 92093, USA

[8]Department of Bioengineering, Stanford University, Stanford, CA 94305, USA

Abstract

An effective method for direct chemical control over the production of specific proteins would be widely useful. We describe Small Molecule-Assisted Shutoff (SMASh), a technique in which proteins are fused to a degron that removes itself in the absence of drug, leaving untagged protein. Clinically tested HCV protease inhibitors can then block degron removal, inducing rapid degradation of subsequently synthesized protein copies. SMASh allows reversible and dose-dependent shutoff of various proteins in multiple mammalian cell types and in yeast. We also used SMASh to confer drug responsiveness onto a RNA virus for which no licensed inhibitors exist. As SMASh does not require permanent fusion of a large domain, it should be useful when control over protein production with minimal structural modification is desired. Furthermore, as SMASh only involves a single genetic modification and does not rely on modulating protein-protein interactions, it should be easy to generalize to multiple biological contexts.

Correspondence should be addressed to M.Z.L. (mzlin@stanford.edu).

AUTHOR CONTRIBUTIONS

H.K.C. optimized SMASh and performed mammalian cell, yeast, and virus experiments, and wrote the manuscript. C.L.J. performed mammalian cell experiments and contributed to the manuscript. J.Y. optimized SMASh and performed mammalian cell experiments. Y.H. performed mammalian cell experiments. S.A.K. packaged virus. R.K.P. packaged virus and provided advice. R.Y.T. provided advice. M.Z.L. designed SMASh, performed mammalian cell experiments, directed the project, and wrote the manuscript.

COMPETING FINANCIAL INTERESTS

The authors declare no competing financial interests.

Technology for rapidly shutting off the production of specific proteins in eukaryotes would be widely useful in research and in gene and cell therapies, but a simple and effective method has yet to be developed. Controlling protein production through repression of transcription is slow in onset, as previously transcribed mRNA molecules continue to produce proteins. RNA interference (RNAi) induces mRNA destruction, but RNAi is often only partially effective and can exhibit both sequence-independent and sequence-dependent off-target effects[1]. Furthermore, mRNA and protein abundance are not always correlated due to translational regulation of specific mRNAs[2-4]. Lastly, both transcriptional repression and RNAi take days to reverse[5,6].

To address these limitations, we wished to devise a method for chemical regulation of protein expression at the post-translational level. An ideal method would feature 1) genetic specification of the target protein, 2) a single genetic modification for simplicity, 3) minimal modification of the expressed protein, 4) generalizability to many proteins and cell types, and 5) control by a drug with proven safety and bioavailability in mammals. While methods have been devised with some of these characteristics (**Supplementary Results, Supplementary Table 1**), none have encompassed all of them. We envisioned that a degron that removes itself in a drug-controllable manner could serve as the basis for a new method with all the desired features. In particular, we reasoned that if a site-specific drug-inhibitable protease and a degron were fused to a protein via an intervening protease site, then by default the protease and degron would be removed and the protein expressed. However, in the presence of protease inhibitor, the degron would remain attached on new protein copies, causing their rapid degradation (**Fig. 1a**).

Here, we show that a system of this design using hepatitis C virus (HCV) nonstructural protein 3 (NS3) protease enables clinically tested drugs to effectively shut off expression. We termed this method “small-molecule assisted shutoff”, or SMASh. SMASh enabled drug-induced suppression of various proteins in multiple eukaryotic cell types. In contrast to other single-component methods of post-translational regulation of protein expression, SMASh functions robustly in yeast as well. Finally, we used SMASh to confer HCV protease inhibitor sensitivity onto an RNA virus currently in clinical trials for cancer but for which no licensed drug inhibitor exists. SMASh thus enables post-translational regulation of protein production with rapid onset and minimal protein modification in a broad array of experimental systems, while requiring only a single genetic modification, the addition of the SMASh tag to the coding sequence of interest.

RESULTS

The SMASh tag, a drug-controllable self-removing degron

We previously used HCV NS3 protease to control protein tagging with drugs[7,8] because it is monomeric, highly selective, and well inhibited by non-toxic cell-permeable inhibitors such as simeprevir, danoprevir, asunaprevir, and ciluprevir, some of which are clinically available[9-12]. We hypothesized that we could use NS3 protease fused in *cis* to remove degrons from proteins of interest shortly after translation by default, then apply inhibitor to block degron removal on subsequently synthesized copies. If the degron is sufficiently strong, then inhibitor would cause new proteins to be rapidly degraded, in effect shutting off

further production. We refer to this strategy as Small Molecule-Assisted Shutoff, or SMASh (**Fig. 1a**).

During the development of tags for newly synthesized proteins called TimeSTAMPs[7], we cloned a sequence encoding the NS3 protease domain (hereafter, NS3pro) followed by NS4A (**Fig. 1b**). We noticed that mouse PSD95 protein connected to NS3pro via a substrate sequence was expressed in HEK293 cells, both when self-removal of NS3pro was allowed to occur and when removal was inhibited by asunaprevir (**Fig. 1c**). However, when fused via the same sequence to NS3pro followed by NS4A, PSD95 was well expressed only in the absence of asunaprevir, but was poorly expressed in its presence (**Fig. 1c**).

To explain these results, we surmised that the arrangement of NS3pro and NS4A sequences in our construct had created a functional degron. During HCV replication, the free NS4A N-terminus forms a hydrophobic α-helix that is inserted into the endoplasmic reticulum membrane[13] (**Supplementary Fig. 1a**). This N-terminus is created by cleavage of the HCV nonstructural polypeptide at the NS3/4A junction (**Supplementary Fig. 1a**) due to its positioning in the protease active site by the NS3 helicase domain[14]. Our engineered construct lacks the helicase domain, so NS3/4A cleavage may not occur (**Supplementary Fig. 1b**). The hydrophobic sequences of NS4A, unable to insert into the membrane without a free N-terminus, might then exhibit degron-like activity.

We tested the role of these putative destabilizing elements in suppressing expression of jellyfish yellow fluorescent protein (YFP) fused to the self-removing NS3pro-NS4A cassette. In the absence of asunaprevir, a 30-kDa YFP fragment was released as expected (**Fig. 1d**). In contrast, with asunaprevir, virtually no full-length 64-kDa YFP-NS3pro-NS4A fusion was detected (**Fig. 1d**), similar to the earlier observations with PSD95. Mutation of a 41-residue stretch comprising putatively unstructured sequence from NS3 helicase and hydrophobic sequence from NS4A (dotted line in **Fig. 1b**) to glycines and serines rescued expression of the full-length protein in drug to levels similar to YFP expressed without drug (**Fig. 1d**). These results indicate that an unstructured hydrophobic sequence derived from NS3 helicase and NS4A triggers rapid degradation of fused proteins.

We next examined which proteolytic pathways were responsible for degrading NS3pro-NS4A fusions. We allowed cells expressing YFP-NS3pro-NS4A to produce uncleaved YFP-NS3pro-NS4A in asunaprevir while applying inhibitors of proteasome or autophagosome degradation (**Supplementary Fig. 1c**). Proteasome inhibition (by MG132 or bortezomib) or autophagy inhibition (by chloroquine or bafilomycin A1) each modestly increased YFP-NS3pro-NS4A protein levels (**Supplementary Fig. 1c**). However, combined inhibition of the proteasome and the autophagosome (by MG132 and chloroquine) rescued YFP-NS3pro-NS4A expression to the same level as the mutant in which unstructured and hydrophobic amino acids were replaced with a glycine-serine linker (**Supplementary Fig. 1c**). This was not restricted to YFP fusions, as a PSD95-NS3pro-NS4A fusion was similarly affected (**Supplementary Fig. 1d**). These findings suggest that the NS3pro-NS4A cassette harbors a bifunctional degron capable of both proteasomal and lysosomal degradation.

To summarize our results so far, proteins fused to the NS3 protease-NSA cassette via a substrate sequence were well expressed in the absence of protease inhibitor at the size expected for released protein. By contrast, in the presence of protease inhibitor, steady-state levels of the fusion protein were drastically reduced. This implies that fusion of a NS3pro-NS4A cassette with an intervening protease site would allow NS3 inhibitor application to effectively stop further protein production, as desired for our SMASh scheme (**Fig. 1a**). We thus designated the cassette comprising the NS3 protease domain, NS4A, and a *cis*-cleavage site as a "SMASh tag".

SMASh functions on either terminus

In the above constructs, the SMASh tag was fused at the C-termini of proteins. We next optimized the ability of the SMASh tag to remove itself from an N-terminal location. Adding linker sequences and using a faster protease cleavage site proved optimal for self-removal of an N-terminal SMASh tag from the mouse Arc protein while preserving drug responsiveness (**Supplementary Fig. 2a**). The final N-terminal SMASh tag regulated Arc with similar efficacy as the C-terminal SMASh tag (**Supplementary Fig. 2b,c**). To further confirm that SMASh tags robustly regulate proteins from either terminus, we coexpressed SMASh-YFP or YFP-SMASh in HEK293 cells. In the absence of asunaprevir, YFP was liberated from either N-terminal or C-terminal fusions, while YFP protein levels were significantly reduced in drug (**Fig. 2a**). Fluorescence imaging of living cells confirmed this effect, with YFP nearly undetectable in the presence of asunaprevir (**Fig. 2b**). Drug did not affect expression of an untagged cotransfected red fluorescent protein, showing the selectivity of asunaprevir for the SMASh-tagged target.

SMASh allows tunable, reversible, and rapid control

To determine whether SMASh allows tunable control of protein levels, we treated cells expressing YFP-SMASh with asunaprevir at concentrations from 15 pM to 15 μM. YFP levels were regulated by asunaprevir in a clear dose-dependent manner (**Fig. 3a,b**). The 50% effective concentration (EC_{50}) of asunaprevir as measured by YFP suppression was approximately 1 nM, comparable to the EC_{50} in HCV replicon assays[11], demonstrating that binding of drug to NS3 protease is unaltered in the SMASh construct. Notably, YFP was undetectable with asunaprevir at 1.5 μM, a concentration at which it exhibits no activity against cellular proteases and is not cytotoxic[11]. Asunaprevir achieved protein repression to 1.9% of undrugged levels at 150 nM, a concentration that can be maintained in plasma and organs for hours following ingestion of non-toxic doses in humans, dogs, and rodents[11,15]. Thus SMASh-mediated repression is tunable with > 50-fold dynamic range using drug concentrations that are non-toxic and achievable *in vivo*.

Because HCV protease inhibitor prevents accumulation of new protein copies without affecting old copies, levels of target proteins following shutoff depend on their degradation rate. Interestingly, SMASh enables easy measurement of protein half-lives, as the liberated species is no longer produced after drug addition, allowing decay to be followed by immunoblotting. This is similar to how cycloheximide is often used to block all protein synthesis for measuring protein decay rates, but unlike cycloheximide, SMASh-mediated shutoff is specific to the tagged protein. We used SMASh to measure half-lives in HEK293

cells of the relatively long-lived and short-lived proteins PSD95 and human CYP21A2, respectively, as 12.4 h and 2.4 h (**Supplementary Fig. 3a, 4a**). Next, we characterized how quickly proteins with a retained SMASh tag are degraded compared to their untagged state. Using a simple mathematical model relating observed relative abundances of protein species to synthesis and degradation rates (**Methods**), we found that the SMASh tag reduced the half-life of PSD95 from 12.6 h to 1.1 h (**Supplementary Fig. 3b**) and of CYP21A2 from 144 min to 15 min (**Supplementary Fig. 4b**).

As mRNA transcripts are not affected by protease inhibitor treatment, protein shutoff by SMASh should be readily reversible upon drug removal. To test this, we incubated HeLa cells expressing YFP-SMASh for 12 h post-transfection with asunaprevir to ensure initial shutoff. Then, after drug washout, we followed the appearance of YFP over time. By immunoblotting, YFP signal appeared within 1 h (**Fig. 3c**). By live-cell fluorescence microscopy, YFP signal was visible within 2 h (**Fig. 3d**). The slower appearance of YFP by fluorescence is consistent with the maturation kinetics of YFP, which has a time constant of 40 min[16].

Taken together, our results demonstrate that SMASh can control protein expression in a dose-dependent and reversible manner by causing rapid degradation of tagged proteins synthesized in the presence of drug. Recovery of protein expression after drug removal is rapid as mRNA pools are not depleted, which allows fast onset of protein production.

SMASh functions on multiple protein types and in neurons

We next determined if SMASh can control production of a variety of protein types. SMASh was able to control a multimeric enzyme, mouse calcium/calmodulin-activated protein kinase IIα(**Fig. 4a**), and a multi-pass transmembrane protein, the *Drosophila* GluRIIA glutamate receptor (**Fig. 4b**). Additionally, SMASh was able to control a short-lived protein, CYP21A2 (half-life ~2 h, **Fig. 4c**). Thus, for the six proteins of various sizes and structures which we tested – PSD95, YFP, Arc, CaMKIIα, GluRIIA and CYP21A2 – the SMASh tag conferred robust drug control.

Synthesis of specific proteins is tightly regulated by growth factors and synaptic activity in neurons, where it is required for long-lasting cellular changes that support memory formation. As our previous experiments using SMASh were only performed in proliferating cell types, we therefore investigated whether SMASh could function in post-mitotic neurons as well. We indeed observed that SMASh conferred drug control over the production of YFP in primary cultures of rat and mouse cortical/hippocampal neurons (**Supplementary Fig. 5a, b**).

SMASh functions in yeast

We next tested the SMASh tag in budding yeast. Yeast genes can be regulated with drug-responsive promoters, but this requires expression of an exogenous transcription factor from another gene and abrogates endogenous transcriptional regulation[17]. Yeast protein stability can be regulated by a temperature-sensitive degron, but this induces a heat shock response and requires switching growth media[18]. Among methods to control protein stability with

drugs, the only one to be successfully adapted to yeast is the auxin-induced degradation (AID) method, which involves attaching proteins of interest to a domain that recruits an ubiquitin ligase in an auxin-dependent manner[18,19]. However, AID requires permanent tagging of the protein of interest and expression of a second transgene, and can exhibit premature auxin-independent degradation or incomplete auxin-dependent degradation[18]. Thus, a method for drug regulation of protein production that is simpler and more robust would be desirable in yeast.

When expressed in yeast from an episomal gene, we found the C-terminal SMASh tag was able to suppress YFP expression in drug, as it did in mammalian cells (**Supplementary Fig. 6a**). However, the N-terminal SMASh tag optimized for mammalian cells showed leaky expression of YFP in drug (data not shown). Reverting the cleavage site to a slower-cleaving site fixed this problem (**Supplementary Fig. 6a**), perhaps due to HCV protease being more active at the 30 °C growth temperature for yeast than at 37° C. SMASh was able to repress YFP expression to undetectable levels at 3 μM asunaprevir (**Supplementary Fig. 6a-c**), regardless of the absence or presence of drug efflux pumps[20] (**Supplementary Fig. 6a**). These results demonstrate that SMASh confers robust drug-mediated control of protein expression in yeast using micromolar drug concentrations. To the best of our knowledge, SMASh is the first method requiring only a single genetic modification to impose drug control over the expression of specific proteins in yeast.

We next determined whether SMASh can regulate the production of proteins encoded by single-copy chromosomal genes in yeast. First, we expressed YFP-SMASh from an integrated chromosomal location and again observed robust suppression of protein levels by drug (**Fig. 5a, b**). Next, we integrated the SMASh tag at the ends of endogenous genes encoding YSH1, an endoribonuclease which confers a temperature-dependent growth phenotype when repressed[21], and SEC14, an essential phosphatidylinositol/phosphatidylcholine transfer protein. YSH1-SMASh yeast growth was normal in the absence of drug but suppressed in the presence of drug, with the effect more pronounced at 37 °C (**Fig. 5c**). The ability of SMASh to control YSH1 suggests that degradation of SMASh tags in yeast can occur considerably faster than the 30-45-min half-life of YSH1[22]. SEC14-SMASh yeast growth was also normal in the absence of drug, but was robustly suppressed in the presence of drug at the standard growth temperature of 30 °C (**Fig. 5d**). We also used SEC14-SMASh yeast to test C-terminal SMASh tag function at 23 °C, a temperature used by other model organisms such as *Drosophila* or *C. elegans.* We observed that SMASh functions at 23 °C as well, enabling wild-type levels of growth without drug and complete suppression with drug, implying that both cleavage and suppression are effective at 23 °C. In summary, SMASh functions in yeast to regulate episomal and chromosomal transgenes and tagged endogenous genes at temperatures from 23 to 37 °C.

SMASh enables pharmacological control over an RNA virus

Many RNA viruses infect and lyse tumor cells more efficiently than normal cells[23]. These viruses, which include measles virus (MeV) and vesicular stomatitis virus, are under active clinical investigation as oncolytic agents[23]. While currently tested agents are nonpathogenic, safety will become a concern if they are engineered for enhanced cytotoxicity or immune

evasion as has been proposed[23-25], or if they are used in immunocompromised patients. It may thus be crucial to develop drug-triggered off-switches. However, there are no clinically available inhibitors for most RNA virusess. Furthermore, regulation through drug-dependent transcription is not possible with pure RNA viruses, as their life cycles bypass DNA replication and transcription. As SMASh regulates protein production directly, we explored the possibility that it could be used as an off-switch to enhance the safety of RNA virus-based therapies.

As MeV is most advanced in clinical testing[25], we chose to create a SMASh-controlled MeV as a model for engineering drug control into viral therapies. MeV phosphoprotein (P) brings the viral large (L) protein, a RNA-dependent RNA polymerase, to the nucleoprotein (N)-encapsidated viral genome. We hypothesized that tagging P with SMASh would allow HCV protease inhibitors to block MeV replication (**Fig. 6a**). We chose to fuse the P C-terminus to SMASh, as this seemed less likely to affect production of the infectivity factor C protein, which occurs from an overlapping open reading frame beginning 19 nucleotides downstream of the P start codon[26]. To inhibit viral replication, drug control of P expression needs to be rapid. We thus first performed a drug chase to determine P stability (**Supplementary Fig. 7a**). We observed that P protein produced from P-SMASh without drug decayed noticeably after 3 h in asunaprevir, indicating that P is relatively short-lived (**Supplementary Fig. 7b**). We also measured the tightness of shutoff by specifically labeling protein synthesized after inhibitor addition with the methionine analog azidohomoalanine (AHA), followed by click chemistry and purification. Immunoblotting revealed no AHA-labeled P or P-SMASh from cells incubated with AHA and asunaprevir simultaneously (**Supplementary Fig. 7b**), indicating that inhibitor suppressed accumulation of newly synthesized P to undetectable levels. AHA labeling and purification did detect P in the absence of protease inhibitor (**Supplementary Fig. 7b**), confirming the efficacy of the labeling and purification steps. These data demonstrate that further production of SMASh-tagged P protein can be robustly shut off by protease inhibitor.

Finally, to make MeV drug-controllable, we replaced the P coding region with P-SMASh in MeV-EGFP, which also expresses enhanced green fluorescent protein (EGFP)[27], creating MeV-EGFP-P-SMASh (**Fig. 6b**, **Supplementary Fig. 8a**). In the absence of asunaprevir, MeV-EGFP-P-SMASh replicated to a similar titer as parental MeV-EGFP in Vero cells (MeV-EGFP-P-SMASh 1.5×10^7 $TCID_{50}$/ml vs MeV-EGFP 3.8×10^7 $TCID_{50}$/ml, measured by end-point dilution), indicating functionality of liberated P in viral replication. MeV-EGFP-P-SMASh also expressed EGFP and induced formation of syncytia as efficiently as parental MeV-EGFP in the absence of drug (**Fig. 6c**). In contrast, in the presence of drug, EGFP expression and formation of syncytia by MeV-EGFP-P-SMASh was completely abolished, while parental MeV-EGFP virus was unaffected (**Fig. 6c**). Suppression was remarkably tight, with drug suppresssing 97.3% of EGFP fluorescence compared to the untreated case 3 days post-transfection (**Fig. 6d, Supplementary Fig. 8b**). Immunoblotting confirmed that asunaprevir efficiently inhibited P production in virus-infected cells (**Fig. 6e**). Thus, in summary, SMASh allowed us to render MeV exquisitely sensitive to inhibition by HCV NS3 protease inhibitors. Through the simple insertion of a SMASh tag in one viral

gene, we were able to create a drug-regulatable version of this RNA virus for which no specific clinically approved inhibitors previously existed.

DISCUSSION

We have presented a new concept, SMASh, for drug regulation of protein production. SMASh is unique in combining multiple desirable features, including rapid onset, reversible and robust drug regulation of protein expression, a requirement for only a single genetic modification, minimal modification to proteins of interest, and use of a clinically approved drug. SMASh satisfies a long-standing need for a simple generalizable method for reversible drug control of protein production while allowing protein expression with minimal perturbation[28].

Earlier strategies to control specific protein levels via drug-dependent degradation or stabilization either substantially change target protein structure or require multiple components (**Supplementary Table 1**). Domains that are unstable in the absence[29-31] or presence[32,33] of drug binding allow chemical control of protein abundance, and like SMASh, function autonomously as single genetic tag. However, unlike SMASh, these fusions are permanent. The AID system of drug-induced destabilization requires both the attachment of a large domain and co-expression of a second protein[18]. As fusion to small peptides preserves protein function in some cases where GFP does not[34], SMASh should be less likely to perturb function than methods that permanently attach large domains. For example, both termini of MeV P protein are believed to interact with N protein[35,36], and P-GFP and GFP-P fusions block and severely hinder MeV replication[37], respectively. By contrast, MeV expressing P-SMASh replicated similarly to parental virus. Minimal protein modification may also be useful in yeast, as attachment of long protein sequences may adversely affect a large percent of yeast proteins. For instance, among 2086 yeast proteins whose localization was studied by fusion to a 237-residue green fluorescent protein (GFP) tag or a 93-residue tag containing multiple hemagglutinin (HA) epitopes, a large proportion, 32%, showed different localizations with the two tags, suggesting that at least one of the tags caused protein mislocalization[38].

Earlier methods to control the production of untagged proteins using established drugs also have limitations in complexity, performance, or generalizability. In SURF, drug-induced ubiquitin fragment complementation triggers degron removal from the C-terminus of a protein of interest, which can be traceless if the native C-terminus is accessible to ubiquitin hydrolases[39]. However, SURF involves a target protein fusion plus expression of a complementation partner, and is leaky unless components are further regulated by drug-inducible transcription, which then necessitates expression of the drug-regulated transcription factor as a third protein and the use of a second drug[40]. Ubiquitin ligases have been fused to protein-binding domains to recognize specific targets including unmodified endogenous proteins[41], with temporal regulation supplied by drug-inducible transcription. This approach thus also requires two components, the fusion protein and a drug-regulated transcription factor, and implementation depends on the availability of targeting domains for proteins of interest. Notably, the nature of chemical regulation in this system is purely transcriptional. As SMASh control is faster than transcriptional regulation, it can be used in

place of drug-regulated transcription to improve the performance of the above methods. However, it may be easier to simply tag the protein of interest directly with SMASh, obviating the need for other genetic modifications. Indeed, recently developed genome editing technologies may enable tagging of endogenous genes with SMASh in various cell types.

Finally, one method, PROTACS, does not require any artificial protein expression at all, using bivalent small molecules to bring ubiquitin ligases to protein targets[42]. However, in PROTACS, small molecules must be developed for each protein target if they do not exist already. Generation of small molecules that are non-toxic in cells and animals, and specific for a protein target, is not assured for a given protein. Each new case would require an extensive drug development effort, rendering this approach not easily generalizable.

Indeed, a notable feature of SMASh is that it uses HCV protease inhibitors, which are already approved for long-term use in humans. SMASh uses drug concentrations achievable *in vivo* in mammals without toxicity, in contrast to some other techniques[33,43]. Our experiments also indicate that asunaprevir is able to efficiently cross the yeast cell wall. Even when transcribed from episomes with the strong GPD promoter, SMASh-tagged YFP levels were completely suppressed by 3 μM asunaprevir. In contrast, 1000 μM auxin was required for AID to suppress a protein expressed from the ten-fold weaker ADH promoter[18,44].

SMASh differs from most other strategies for regulating protein stability in that it selectively controls the degradation of new copies of a protein of interest, and not pre-existing copies. Cells respond rapidly to environmental stimuli such as growth signals[45] or, in the nervous system, synaptic activity[7], by synthesizing new proteins. SMASh can be used to query the role of specific new protein species in such biological responses. SMASh can also be used to estimate half-lives of proteins of interest, as the persistence of untagged protein copies previously produced in the absence of drug can be measured over time while further production is inhibited in the presence of drug. Here, SMASh can be used similarly to cycloheximide or anisomycin in estimating protein half-lives[46], but with much less toxicity. Cycloheximide and anisomycin, by inhibiting all protein synthesis in the cell, can be expected to impair cell health and to generate erroneous half-life calculations as levels of proteins regulating the stability of the protein of interest also drop. The SMASh system may thus be especially advantageous for measuring half-lives of long-lived proteins such as PSD95 (**Supplementary Fig. 3a**).

SMASh also allows rapid increases in protein levels. Expression of a protein can be repressed with drug, then when expression is desired, the drug can be washed out. Protein will then immediately accumulate from ongoing translation of existing mRNAs. Upregulating proteins by reversing SMASh shutoff should be faster than by inducing gene transcription, which takes many hours in mammalian systems[47].

RNA viruses that replicate more efficiently in certain neoplastic cell types have long been considered as targeted cancer treatments. However, only viruses that cause non-pathogenic or mild disease, such as vaccine-strain MeV, are currently being tested in clinical trials. As

the self-limited nature of these viruses will likely limit their oncolytic efficacy, researchers have proposed modifying them to increase cytotoxicity or immune evasion[48,49]. As such steps could lead to unexpected side effects[50], it would be desirable to have pharmacological methods for terminating replication of engineered viruses[24]. We found that SMASh enabled robust control by HCV NS3 protease inhibitors over MeV, for which no clinically available specific inhibitors exist. We expect that other viruses can be controlled by SMASh-tagging as well.

In summary, SMASh has advantages over other methods for controlling levels of proteins of interest in minimizing protein modification, requiring only one genetically encoded modification, and using clinically available drugs that are nontoxic and cell permeable. Furthermore, SMASh functions robustly in mitotic and non-mitotic mammalian cells, and also in yeast. Using SMASh, we have also engineered, for the first time, an RNA virus that can be tightly regulated by a drug without the need to develop new, virus-specific small molecule inhibitors. Thus, with its ease of implementation and generalizability, the SMASh technique can be applied to a variety of problems in biomedicine and biotechnology, ranging from the study of gene function to the engineering of drug-dependent features in cellular and viral therapies.

ONLINE METHODS

DNA constructs

Plasmids encoding PSD95 or Arc fused to TimeSTAMP cassettes[17,18] were modified by standard molecular biology techniques including PCR, restriction enzyme digestion and ligation or In-Fusion enzyme (Clontech) to create new TimeSTAMP variants or SMASh variants. All subcloned fragments were sequenced in their entirety to confirm successful construction. Full sequences of all plasmids used in this study are available upon request.

Cell culture and transfection

HEK293 (Life technologies), Vero (ATCC), and HeLa (kind gift from Dr. Mark Kay at Stanford Univ.) cell lines were cultured at 37°C in 5% CO_2 in Dulbecco's Modified Eagle's Medium (DMEM, HyClone) supplemented with 10% fetal bovine serum (Gibco), 2 mM glutamine (Life Technologies) and 100 U/mL penicillin and 100 μg/mL streptomycin (Life Technologies). Cells were transfected using Lipofectamine 2000 (Life Technologies) in Opti-MEM (Life Technologies) according to the manufacturer's recommended protocol.

Chemical reagents

HCV NS3 inhibitors ciluprevir (CLV) and asunaprevir (ASV) were obtained by custom synthesis (Acme Bioscience) and dissolved in DMSO (Thermo) at 3 mM for medium-term storage at −20°C. These were then diluted into media to achieve the desired final concentration (1-3 μM) for treatment of cells. Further serial dilutions were performed for the dose-dependency experiment. For long-term CLV and ASV incubations, drug was applied simultaneously with transfection media or 1-2 h after transfection. MG132 (Sigma) was dissolved in DMSO for a 1000X working stock of 10 mM. Bortezomib (Adooq Biosci.) was dissolved in DMSO for a 500X working stock of 33 μM. Chloroquine diphosphate salt

(Sigma) was dissolved in H2O for a 1000X (100 mM) working stock. Bafilomycin A1 (Santa Cruz) was dissolved in DMSO for a 500X (100 μM) working stock. Azidohomoalanine (AHA) (Click-IT, Invitrogen) was dissolved in DMSO for a 500X working stock of 25 mM. Alkyne-PEG4-biotin (Invitrogen) was dissolved in DMSO for a 100X working stock of 4 mM. L-cystine dihydrochloride (Sigma) was dissolved in H2O pH 2.0 for a working stock of 0.1 M.

Yeast strains and cell growth

All experiments were carried out in the w303-1A ADE2+ strain background[51] and a pump-deficient w303-1A strain (MATa can1-100, his3-11,15, leu2-3,112, trp1-1, ura3-1, ade2-1, pdr1::kanMX, pdr3::kanMX)[20]. SMASh strains were made by transformation of yeast episomal plasmid (pAG426) and yeast integrating plasmid (pRS405), expressing SMASh fused YFP under GPD promoter Yeastmaker DNA kit (Clontech) was used for yeast Li-Acetate transformations. Cells were grown at 30 °C in SD media or YDP media. To generate SMASh knock-in yeast, PCR fragments containing SMASh tag followed by yeast ADH1 terminator and NatMX (clonNAT resistance gene) are inserted before the termination codon of the protein of interest by homologous recombination. To perform yeast spotting assay, YDP plates were prepared with ASV or the same concentration of DMSO (1% v/v).

Primary neuronal culture

All animal procedures were approved by the Stanford University Administrative Panel on Laboratory Animal Care, and were performed in accordance with the applicable regulatory standards. Sprague-Dawley rat E15 cortico-hippocampal tissue and FVB mouse E18 cortical tissue were dissected, incubated in RPMI (Life Technologies) with papain (Worthington) and DNase I (Roche) for dissociation, triturated, and electroporated using the Amaxa Rat or Mouse Neuron Nucleofector kit (Lonza), before being plated on poly-L-lysine-coated 4-chamber 35-mm glass bottom dishes (In Vitro Scientific), in the presence of 5-10% FBS (Gibco), at a density of ~150K neurons per quadrant. Neurons were cultured in NeuroBasal media (Life Technologies) supplemented with GlutaMAX, B-27, and Pen-strep (Life Technologies) at 37°C with 5% CO2. Every 3 days, 50% of media was refreshed.

Virus cloning, packaging and infection

To construct p(+)-MeV-EGFP-PSMASh, DNA encoding the SMASh tag was added in frame to the P open reading frame in p(+)-MeV-EGFP, the resulting full-length clone corrected for the paramyxovirus rule-of-six, and verified through sequencing. Recombinant MeV were recovered using a modified rescue system[52]. BSR-T7/5 cells[53] were transfected with p(+)-MeV-EGFP or p(+)-MeV-EGFP-PSMASh, respectively, and plasmids encoding the L, N, or P proteins derived from the MeV IC-B strain[54]. All constructs were under the control of the T7 promoter. 48 h post-transfection, BSR-T7/5 helper cells were overlaid on Vero cells stably expressing human CD150 and SLAM[55], and overlay plates incubated at 32°C until infectious centers became detectable. Virions from individual centers were transferred to fresh Vero-SLAM cells for generation of passage two virus stocks. To confirm integrity of recombinant viruses, RNA was extracted from infected cells using the RNeasy mini kit (Qiagen) and cDNAs created using random hexamer primers and Superscript III reverse transcriptase (Life Technologies). PCR was performed with primers 28-F:

TAATCTCCAAGCTAGAATC and 35-R: AGCCTGCCATCACTGTA (**Supplementary Fig. 9**) and sequenced. To prepare virus stocks, Vero cells were infected at an MOI of 0.01 $TCID_{50}$/cell with the relevant virus and incubated at 32°C until cytopathic effect (CPE) become detectable. Plates were then moved to 37°C and incubated until 100% CPE. Cells were scraped in Opti-MEM (Life Technologies), and particles released by two freeze-thaw cycles. Titers were determined by $TCID_{50}$ titration on Vero cells according to the Spearman-Karber method as described[56]. Virus infection for drug controllability tests was initiated through inoculation of Vero cells at an MOI of of 0.1 and 1 $TCID_{50}$/cell at 32°C.

Microscopy

For imaging of MeV-infected cells, brightfield and fluorescence microscopy was performed on a Nikon TE300 with a 10×/0.25-numerical aperture (NA) objective. HEK293A cells were imaged with a 20×/0.15 NA objective on the same microscope. The cells were cultured in 12-well plates (Greiner), MeV-infected cells were imaged in culture media (10% FBS supplemented phenol red free DMEM) and HEK293 were imaged in HBSS. Brightfield and fluorescence microscopy of yeast was done with an Olympus 100x/1.4-NA oil immersion objective on Olympus IX80. Yeast cells were imaged in SD media in a ConA (Sigma) coated TC CU109 chamber (Chamlide). For HeLa and neurons, microscopy was performed on a Zeiss Axiovert 200M with a 40×/1.2-NA water immersion objective. These cells were cultured in 4-chamber 35mm glass bottom dishes (In Vitro Scientific) and culture media were replaced with HBSS during live imaging sessions. All microscopes were connected to Hamamatsu ORCA-ER cameras and controlled by Micro-Manager software. Image processing was performed in ImageJ.

Immunoblotting

After washing twice with PBS, cells were lysed with 50-100 µl of hot SDS lysis buffer (100mM Tris HCl pH 8.0, 4% SDS, 20% glycerol, 0.2% bromo-phenol blue, 10% 2-mercaptoethanol) and DNA was sheared by sonication. After heating to 80-90°C for several minutes, cell lysates were loaded onto 4%-12% Bis-Tris gels (NuPAGE, Life Technologies) along with Novex Sharp pre-stained protein standard (Life Technologies) or Precision Plus Protein™ Dual Color Standards (Bio-Rad), dry-transferred to nitrocellulose or PVDF membranes (iBlot system, Life Technologies), probed with primary and secondary antibodies, and imaged using LI-COR Odyssey imaging system. Quantification of immunoblots was performed in ImageJ.

Antibodies

The following primary antibodies were used for immunoblotting at the indicated dilutions: mouse monoclonal anti-PSD95 (NeuroMab, clone K28/43), 1:2000; mouse monoclonal anti-Arc (Santa Cruz, clone C7, sc-17839), 1:200; mouse monoclonal anti-GFP (Pierce, clone GF28R, MA5-15256), 1:1000; rabbit monoclonal anti-GFP (Abcam, clone E385, ab32146), 1:1000; rabbit polyclonal anti-β-actin (GeneTex, GTX124214) 1:10,000; mouse monoclonal anti-GAPDH (Santa Cruz, clone G-9, sc-365062), 1:4000; rabbit polyclonal anti-GAPDH (Santa Cruz, sc-25778), 1:4000; mouse monoclonal anti-GAPDH (Pierce, clone GA1R, MA5-15738), 1:1000; mouse monoclonal anti-measles phosphoprotein (P) (Novus, clone

9H4, NB110-37247 or Abcam, clone 9H4, ab43820), 1:200; rabbit polyclonal anti-CamKIIα (Santa Cruz, sc-13082), 1:200; mouse monoclonal anti-GluRIIA (DSHB, 8B4D2), 1:1000; anti-CYP21A2 (Santa Cruz, clone C-17, sc-48466), 1:200; and rabbit monoclonal anti-HA (Cell Signaling, C29F4), 1:1000. Secondary antibodies were LI-COR 680RD goat-anti-mouse, 680RD goat-anti-rabbit, 800CW goat-anti-mouse, 800CW goat-anti-rabbit, used at 1:5000.

Metabolic labeling, Click chemistry, and pulldown

HeLa cells were cultured in 12-well plates (Greiner) in standard DMEM supplemented with glutamine, pen-strep, and 10% FBS. 20 h after transfection, wells were washed 3x with HBSS, and cells were methionine-depleted via 30 min incubation in metabolic label DMEM [methionine/cystine-free DMEM (Corning Cellgro) supplemented with glutamine, pen-strep, 0.2 mM L-cystine (Sigma), and 10% dialyzed FBS (Thermo)]. Following depletion step, media were replaced with either standard DMEM, metabolic label DMEM with 50 μM AHA, or metabolic label DMEM with 50 μM AHA and 2 μM ASV. Equivalent volumes of DMSO were used as vehicle controls in negative wells. Labeling incubation lasted 3 h, after which each well was washed and lysed with 50 μL gentle lysis buffer [1% SDS, 50 mM Tris HCl pH 8.0, EDTA-free protease inhibitor cocktail (Complete Mini, Roche), phosphatase inhibitor cocktail (Halt, Pierce), 3 μM ASV]. For each condition, lysates from 3 separate wells were pooled. Lysates were sonicated and clarified by centrifugation. For pre-click/pulldown samples, 50 μL of each lysate was reserved and combined with 50 μL of hot SDS lysis buffer for SDS-PAGE analysis.

For click reactions, 50 μL of each lysate was processed using the Click-IT Protein Reaction Buffer kit (Invitrogen) with alkyne-PEG4-biotin (Invitrogen) according to manufacturer's recommendations. Following click labeling, methanol-chloroform extracted protein pellets were resuspended by vortexing in 20 μL of gentle lysis buffer + 80 μL of nondenaturing buffer (1% Nonidet P40, 50 mM Tris HCl pH 8.0, EDTA-free protease inhibitor cocktail). Proteins were allowed to solubilize at 4°C overnight. Biotin-labeled proteins were purified via a magnetic streptavidin bead (PureProteome, Millipore) pulldown. Prior to binding reactions, beads were blocked by incubating 1 hour with 5% BSA solution in PBS, on a rotator at room temp, and washing 3x in PBS-T (PBS plus 0.1% Tween-20). Beads were resuspended in PBS-T. Binding reactions (200 μL volume) proceeded for 1 hour on a rotator at room temp, after which beads were washed 3x with PBS-T. Proteins were eluted for SDS-PAGE by heating beads in 50 μL SDS lysis buffer at 95°C for 10 min.

Calculating half-lives of SMASh-tagged proteins

To calculate production rates of PSD95 and PSD95-SMASh, we assumed that the protein production rate is constant between 24 and 28 h post-transfection, and are the same for PSD95-SMASh protein expressed from a PSD95-SMASh gene with ASV and PSD95 protein expressed from a PSD95-SMASh gene without ASV. The rate of change in protein concentrations can be modeled with the differential equations

$$d\left[PSD95\right](t)/dt = k_{syn,PSD} - k_{deg,PSD95}\left[PSD95\right](t) \quad (1)$$

$$d\left[PSD95SMASh\right](t)/dt = k_{syn,PSDSMASh} - k_{deg,PSD95SMSh}\left[PSD95SMSh\right](t) \quad (2)$$

where [PSD95](*t*) is protein concentration of PSD95 at time t, [PSD95SMASh](*t*) is protein concentration of PSD95-SMASh at time t, $k_{syn,PSD95}$ and $k_{syn,PSD95SMASh}$ are production rate constants of PSD95 and PSD95-SMASh, and $k_{deg,PSD95}$ and $k_{deg,PSD95SMASh}$ are decay rate constants of PSD95 and PSD95-SMASh. Integration of these equations yields

$$\left[PSD95\right](t) = \left(k_{syn,PSD}/k_{deg,PSD95}\right)\left(1 - e^{-k_{deg,PSD95}t}\right) \quad (3)$$

$$\left[PSD95SMASh\right](t) = \left(k_{syn,PSD95SMASh}/k_{deg,PSD95SMASh}\right)\left(1 - e^{-k_{deg,PSD95SMASh}t}\right) \quad (4)$$

We measured PSD95 half-life ($t_{1/2,PSD95}$) by fitting the PSD95 band intensities of different time points to monoexponential decay curves (*n* =3), obtaining 12.6 h. We then determined the decay rate constant of PSD95 ($k_{deg,PSD95} = \ln 2/t_{1/2,PSD95} = 0.055$/h). We defined 1 relative intensity unit (RIU) as the mean band density on immunoblotting from net production of PSD95 in 4h. By immunoblotting lysates from cells incubated for 24 h with ASV then for 4 h without ASV, we obtained a protein amount of 1 RIU for [PSD95](4 h) (standard deviation 0.16, *n* = 3). By immunoblotting in parallel lysates from cells incubated for 24 h without ASV then for 4 h with ASV, we obtained a protein amount of 0.419 RIU for [PSD95SMASh](4 h) (standard deviation 0.07, *n* = 3). With values for $k_{deg,PSD95}$ and for [PSD95](4 h), we then used equation (3) to solve numerically for $k_{syn,PSD95}$, obtaining 0.279 RIU/h. Assuming $k_{syn,PSD95SMASh}$ equals $k_{syn,PSD95}$, we could then use equation (4) to solve numerically for $k_{deg,PSD95SMASh}$, obtaining 0.606/h. The PSD95SMASh half-life $t_{1/2,PSD95SMASh}$ was then calculated as 1.14 h ($t_{1/2,PSD95SMASh} = \ln 2/k_{deg,PSD95SMASh} =$ 1.14 h).

The half-life of CYP21A2-SMASh was calculated from the same equations, except CYP21A2 was substituted for PSD95. Values obtained were: $t_{1/2,CYP21A2} = 2.4$ h, $k_{deg,CYP21A2} = 0.288$/h, [CYP21A2](4 h) = 1 RIU (standard deviation 0.019, n = 3), [CYP21A2SMASh](4 h) = 0.163 RIU (standard deviation 0.025, n = 3), $k_{syn,CYP21A2} = k_{syn,CYP21A2SMASh} = 0.422$/h, $k_{deg,CYP21A2SMASh} = 2.688$/h, $t_{1/2,CYP21A2SMASh} = 0.258$ h.

Supplementary Material

Refer to Web version on PubMed Central for supplementary material.

ACKNOWLEDGMENTS

We thank M. Billeter (University of Zurich) for p(+)-MeV plasmid, Y. Yanagi (Kyushu University) for Vero-SLAM cells, M. Takeda (Kyushu University) for the MeV IC-B strain, J. Glenn (Stanford University) for BILN-2061, and A. Gitler, T. Stearns, A. Morrison, and J. Skotheim, (Stanford University) for yeast plasmids and reagents. We also thank Y. Geng of the Lin laboratory for performing brain dissections, other members of the Lin laboratory for advice, S. Beckwith of the Morrison laboratory for training on yeast procedures, and A. Gitler and G. Sherlock (Stanford University) for critical reading of the manuscript. This work was supported by Stanford Graduate Fellowships (H.K.C. and C.L.J.), a NSF Graduate Research Fellowship (C.L.J.), NIH/NIAID grants 5R01AI071002 and 5R01AI083402 (R.K.P.), NIH/NIGMS EUREKA grant 5R01GM098734 (M.Z.L.), a

Burroughs Wellcome Foundation Career Award for Medical Scientists (M.Z.L.), and an Alliance for Cancer Gene Therapy Young Investigator Award (M.Z.L.).

REFERENCES

1. Sigoillot FD, King RW. Vigilance and validation: Keys to success in RNAi screening. ACS Chem. Biol. 2011; 6:47–60. [PubMed: 21142076]
2. Vogel C, Marcotte EM. Insights into the regulation of protein abundance from proteomic and transcriptomic analyses. Nat. Rev. Genet. 2012; 13:227–232. [PubMed: 22411467]
3. Wu L, et al. Variation and genetic control of protein abundance in humans. Nature. 2013; 499:79–82. [PubMed: 23676674]
4. Battle A, et al. Genomic variation. Impact of regulatory variation from RNA to protein. Science. 2015; 347:664–667. [PubMed: 25657249]
5. Huang CJ, et al. Conditional expression of a myocardium-specific transgene in zebrafish transgenic lines. Dev. Dyn. 2005; 233:1294–1303. [PubMed: 15977161]
6. Matsukura S, Jones PA, Takai D. Establishment of conditional vectors for hairpin siRNA knockdowns. Nucleic Acids Res. 2003; 31:e77. [PubMed: 12888529]
7. Butko MT, et al. Fluorescent and photo-oxidizing TimeSTAMP tags track protein fates in light and electron microscopy. Nat. Neurosci. 2012:1–12.
8. Lin MZ, Glenn JS, Tsien RY. A drug-controllable tag for visualizing newly synthesized proteins in cells and whole animals. Proc. Natl. Acad. Sci. USA. 2008; 105:7744–7749. [PubMed: 18511556]
9. Jiang Y, et al. Discovery of danoprevir (ITMN-191/R7227), a highly selective and potent inhibitor of hepatitis C virus (HCV) NS3/4A protease. J. Med. Chem. 2014; 57:1753–1769. [PubMed: 23672640]
10. Lamarre D, et al. An NS3 protease inhibitor with antiviral effects in humans infected with hepatitis C virus. Nature. 2003; 426:186–189. [PubMed: 14578911]
11. McPhee F, et al. Preclinical Profile and Characterization of the Hepatitis C Virus NS3 Protease Inhibitor Asunaprevir (BMS-650032). Antimicrob. agents chemother. 2012; 56:5387–5396. [PubMed: 22869577]
12. Talwani R, Heil EL, Gilliam BL, Temesgen Z. Simeprevir: a macrocyclic HCV protease inhibitor. Drugs Today (Barc). 2013; 49:769–779. [PubMed: 24524095]
13. Brass V, et al. Structural determinants for membrane association and dynamic organization of the hepatitis C virus NS3-4A complex. Proc. Natl. Acad. Sci. USA. 2008; 105:14545–14550. [PubMed: 18799730]
14. Yao N, Reichert P, Taremi SS, Prosise WW, Weber PC. Molecular views of viral polyprotein processing revealed by the crystal structure of the hepatitis C virus bifunctional protease-helicase. Structure. 1999; 7:1353–1363. [PubMed: 10574797]
15. Yuan L, et al. A rugged and accurate liquid chromatography-tandem mass spectrometry method for the determination of asunaprevir, an NS3 protease inhibitor, in plasma. J. Chromatogr. B Analyt. Technol. Biomed. Life Sci. 2013; 921-922:81–86.
16. Iizuka R, Yamagishi-Shirasaki M, Funatsu T. Kinetic study of de novo chromophore maturation of fluorescent proteins. Anal. Biochem. 2011; 414:173–178. [PubMed: 21459075]
17. Mnaimneh S, et al. Exploration of essential gene functions via titratable promoter alleles. Cell. 2004; 118:31–44. [PubMed: 15242642]
18. Morawska M, Ulrich HD. An expanded tool kit for the auxin-inducible degron system in budding yeast. Yeast. 2013; 30:341–351. [PubMed: 23836714]
19. Nishimura K, Fukagawa T, Takisawa H, Kakimoto T, Kanemaki M. An auxin-based degron system for the rapid depletion of proteins in nonplant cells. Nat. Methods. 2009; 6:917–922. [PubMed: 19915560]
20. Su LJ, et al. Compounds from an unbiased chemical screen reverse both ER-to-Golgi trafficking defects and mitochondrial dysfunction in Parkinson's disease models. Dis. Model Mech. 2010; 3:194–208. [PubMed: 20038714]
21. Garas M, Dichtl B, Keller W. The role of the putative 3' end processing endonuclease Ysh1p in mRNA and snoRNA synthesis. RNA. 2008; 14:2671–2684. [PubMed: 18971324]

22. Belle A, Tanay A, Bitincka L, Shamir R, O'Shea EK. Quantification of protein half-lives in the budding yeast proteome. Proc. Natl. Acad. Sci. USA. 2006; 103:13004–13009. [PubMed: 16916930]
23. Miest TS, Cattaneo R. New viruses for cancer therapy: meeting clinical needs. Nat. Rev. Microbiol. 2014; 12:23–34. [PubMed: 24292552]
24. Russell SJ, Peng KW, Bell JC. Oncolytic virotherapy. Nat. Biotechnol. 2012; 30:658–670. [PubMed: 22781695]
25. Msaouel P, Opyrchal M, Domingo Musibay E, Galanis E. Oncolytic measles virus strains as novel anticancer agents. Expert Opin Biol Ther. 2013; 13:483–502. [PubMed: 23289598]
26. Rima BK, Duprex WP. The measles virus replication cycle. Curr. Top. Microbiol. Immunol. 2009; 329:77–102. [PubMed: 19198563]
27. Zuniga A, et al. Attenuated measles virus as a vaccine vector. Vaccine. 2007; 25:2974–2983. [PubMed: 17303293]
28. Lampson MA, Kapoor TM. Targeting protein stability with a small molecule. Cell. 2006; 126:827–829. [PubMed: 16959558]
29. Banaszynski LA, Chen L-C, Maynard-Smith LA, Ooi AGL, Wandless TJ. A rapid, reversible, and tunable method to regulate protein function in living cells using synthetic small molecules. Cell. 2006; 126:995–1004. [PubMed: 16959577]
30. Iwamoto M, Bjorklund T, Lundberg C, Kirik D, Wandless TJ. A general chemical method to regulate protein stability in the mammalian central nervous system. Chem. Biol. 2010; 17:981–988. [PubMed: 20851347]
31. Stankunas K, et al. Conditional protein alleles using knockin mice and a chemical inducer of dimerization. Mol. Cell. 2003; 12:1615–1624. [PubMed: 14690613]
32. Bonger KM, Chen LC, Liu CW, Wandless TJ. Small-molecule displacement of a cryptic degron causes conditional protein degradation. Nat Chem Biol. 2011; 7:531–537. [PubMed: 21725303]
33. Tae HS, et al. Identification of hydrophobic tags for the degradation of stabilized proteins. Chembiochem. 2012; 13:538–541. [PubMed: 22271667]
34. Andresen M, Schmitz-Salue R, Jakobs S. Short tetracysteine tags to beta-tubulin demonstrate the significance of small labels for live cell imaging. Mol. Biol. Cell. 2004; 15:5616–5622. [PubMed: 15469986]
35. Chen M, Cortay JC, Gerlier D. Measles virus protein interactions in yeast: new findings and caveats. Virus Res. 2003; 98:123–129. [PubMed: 14659559]
36. Shu Y, et al. Plasticity in structural and functional interactions between the phosphoprotein and nucleoprotein of measles virus. J. Biol. Chem. 2012; 287:11951–11967. [PubMed: 22318731]
37. Devaux P, Cattaneo R. Measles virus phosphoprotein gene products: conformational flexibility of the P/V protein amino-terminal domain and C protein infectivity factor function. J. Virol. 2004; 78:11632–11640. [PubMed: 15479804]
38. Huh WK, et al. Global analysis of protein localization in budding yeast. Nature. 2003; 425:686–691. [PubMed: 14562095]
39. Pratt MR, Schwartz EC, Muir TW. Small-molecule-mediated rescue of protein function by an inducible proteolytic shunt. Proc. Natl. Acad. Sci. USA. 2007; 104:11209–11214. [PubMed: 17563385]
40. Lin YH, Pratt MR. A dual small-molecule rheostat for precise control of protein concentration in Mammalian cells. Chembiochem. 2014; 15:805–809. [PubMed: 24615791]
41. Cong F, Zhang J, Pao W, Zhou P, Varmus H. A protein knockdown strategy to study the function of beta-catenin in tumorigenesis. BMC Mol. Biol. 2003; 4(10)
42. Sakamoto KM, et al. Protacs: chimeric molecules that target proteins to the Skp1-Cullin-F box complex for ubiquitination and degradation. Proc. Natl. Acad. Sci. USA. 2001; 98:8554–8559. [PubMed: 11438690]
43. Limenitakis J, Soldati-Favre D. Functional genetics in Apicomplexa: potentials and limits. FEBS Lett. 2011; 585:1579–1588. [PubMed: 21557944]
44. Mumberg D, Muller R, Funk M. Yeast vectors for the controlled expression of heterologous proteins in different genetic backgrounds. Gene. 1995; 156:119–122. [PubMed: 7737504]

45. Shimobayashi M, Hall MN. Making new contacts: the mTOR network in metabolism and signalling crosstalk. Nat. Rev. Mol. Cell. Biol. 2014; 15:155–162. [PubMed: 24556838]
46. Zhou P. Determining protein half-lives. Methods Mol. Biol. 2004; 284:67–77. [PubMed: 15173609]
47. Shoulders MD, Ryno LM, Cooley CB, Kelly JW, Wiseman RL. Broadly applicable methodology for the rapid and dosable small molecule-mediated regulation of transcription factors in human cells. J. Am. Chem. Soc. 2013; 135:8129–8132. [PubMed: 23682758]
48. Cattaneo R, Miest T, Shashkova EV, Barry MA. Reprogrammed viruses as cancer therapeutics: targeted, armed and shielded. Nat. Rev. Microbiol. 2008; 6:529–540. [PubMed: 18552863]
49. Meng X, et al. Enhanced antitumor effects of an engineered measles virus Edmonston strain expressing the wild-type N, P, L genes on human renal cell carcinoma. Mol. Ther. 2010; 18:544–551. [PubMed: 20051938]
50. Chen N, et al. Poxvirus interleukin-4 expression overcomes inherent resistance and vaccine-induced immunity: pathogenesis, prophylaxis, and antiviral therapy. Virology. 2011; 409:328–337. [PubMed: 21071055]
51. Thomas BJ, Rothstein R. Elevated recombination rates in transcriptionally active DNA. Cell. 1989; 56:619–630. [PubMed: 2645056]
52. Brindley MA, et al. A stabilized headless measles virus attachment protein stalk efficiently triggers membrane fusion. J. Virol. 2013; 87:11693–11703. [PubMed: 23966411]
53. Buchholz UJ, Finke S, Conzelmann KK. Generation of bovine respiratory syncytial virus (BRSV) from cDNA: BRSV NS2 is not essential for virus replication in tissue culture, and the human RSV leader region acts as a functional BRSV genome promoter. J. Virol. 1999; 73:251–259. [PubMed: 9847328]
54. Krumm SA, Takeda M, Plemper RK. The measles virus nucleocapsid protein tail domain is dispensable for viral polymerase recruitment and activity. J. Biol. Chem. 2013; 288:29943–29953. [PubMed: 24003217]
55. Ono N, et al. Measles viruses on throat swabs from measles patients use signaling lymphocytic activation molecule (CDw150) but not CD46 as a cellular receptor. J. Virol. 2001; 75:4399–4401. [PubMed: 11287589]
56. Plemper RK, Hammond AL, Gerlier D, Fielding AK, Cattaneo R. Strength of envelope protein interaction modulates cytopathicity of measles virus. J. Virol. 2002; 76:5051–5061. [PubMed: 11967321]

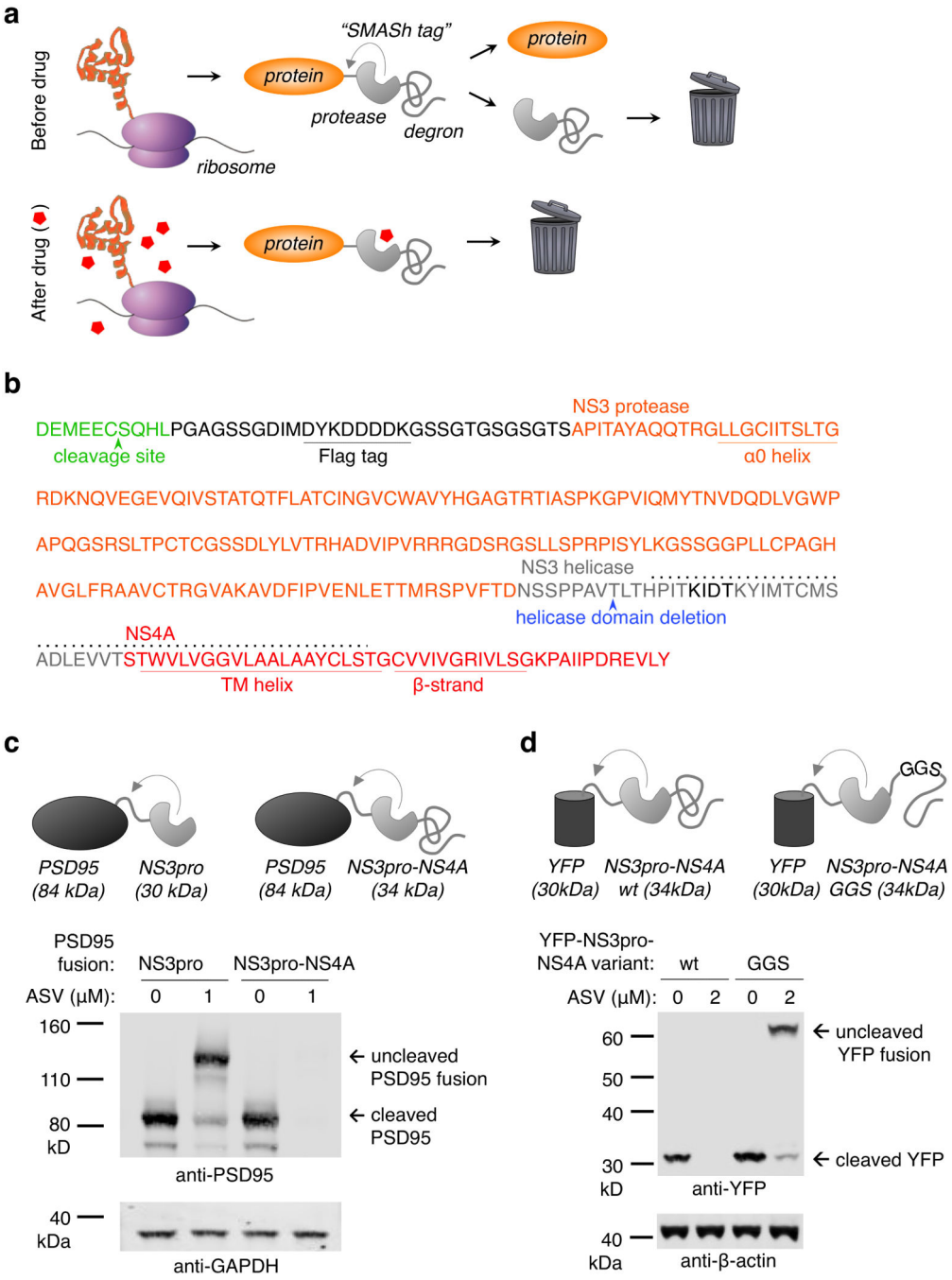

Figure 1.

Small Molecule-Assisted Shutoff (SMASh) concept and development. **(a)** SMASh concept. Top, a target protein is fused to the SMASh tag via a HCV NS3 protease recognition site. After protein folding, the SMASh tag is removed by its internal protease activity, and is degraded due to internal degron activity. Bottom, addition of protease inhibitor induces the rapid degradation of subsequently synthesized copies of the tagged protein, effectively shutting off further protein production. **(b)** Amino acid sequence of the SMASh tag. Sequence derived from NS3 protease (orange), NS3 helicase (gray), and NS4A (red) are

shown. Secondary structures in the context of the original HCV polyprotein are underlined. The NS4A/4B protease substrate (green), has an arrow indicating site of cleavage. Dotted line indicates putative degron region. **(c)** Top, organization of fusions of PSD95 with NS3 protease (NS3pro) or NS3pro-NS4A, with predicted protein fragment sizes indicated. Bottom, in the absence of protease inhibitor asunaprevir (ASV), PSD95 was detectable in HEK293 lysates 24 h post-transfection, for both constructs. With asunaprevir, the PSD95-NS3pro fusion was expressed at full-length size, but the PSD95-NS3pro-NS4A failed to exhibit expression. GAPDH served as a loading control. **(d)** A specific element within NS3pro-NS4A is necessary for degron activity. Transfected HeLa cells expressed either YFP-NS3pro-NS4A, or a variant in which the putative degron (dotted line in **b**) was mutated to a GGS-repeat linker of the same length (GGS), for 24 h with or without ASV. The GGS mutation restores expression in the ASV condition. β-actin served as a loading control.

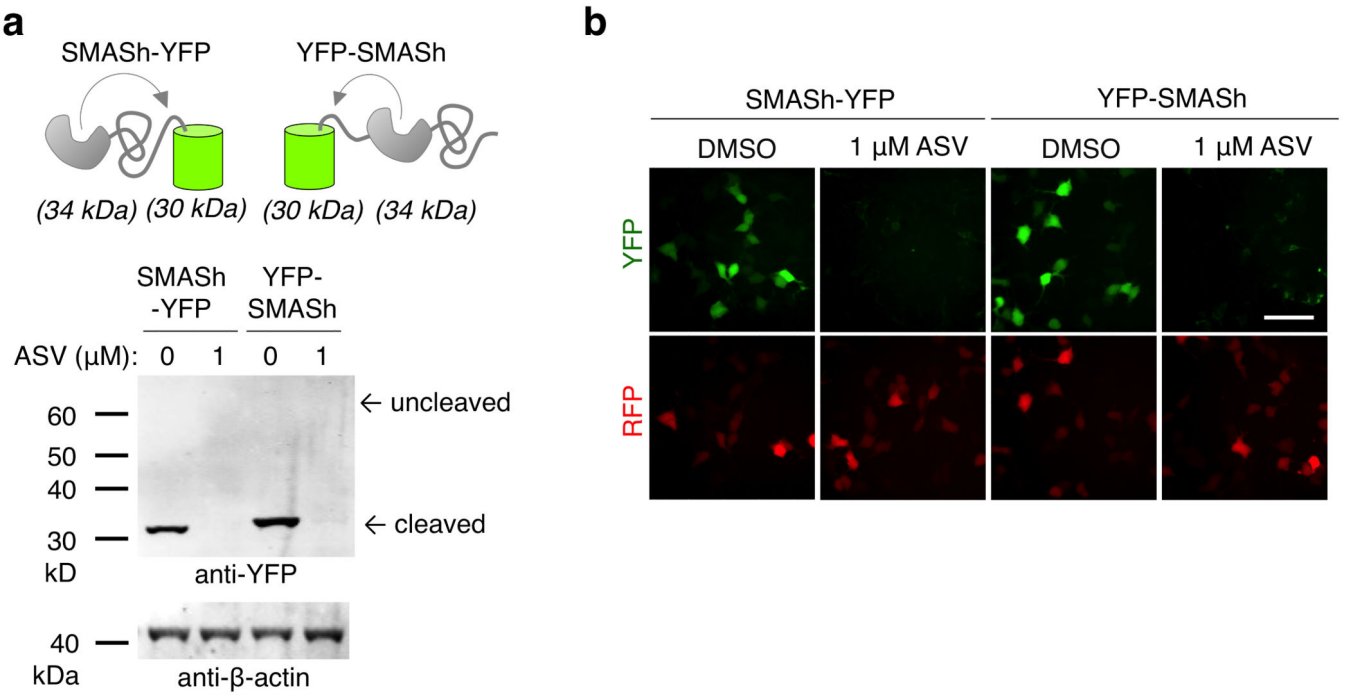

Figure 2.

Proteins can be regulated by SMASh tags at either terminus. **(a)** SMASh can regulate YFP when fused to either terminus. SMASh-YFP or YFP-SMASh were expressed in HEK293 cells in the absence or presence of ASV for 24 h. Immunoblotting revealed shutoff of YFP expression by ASV for both constructs. DMSO was used as vehicle control. β-actin served as a loading control. **(b)** Fluorescence microscopy confirmed shutoff of YFP expression by ASV for both constructs. Scale bar, 50 μm.

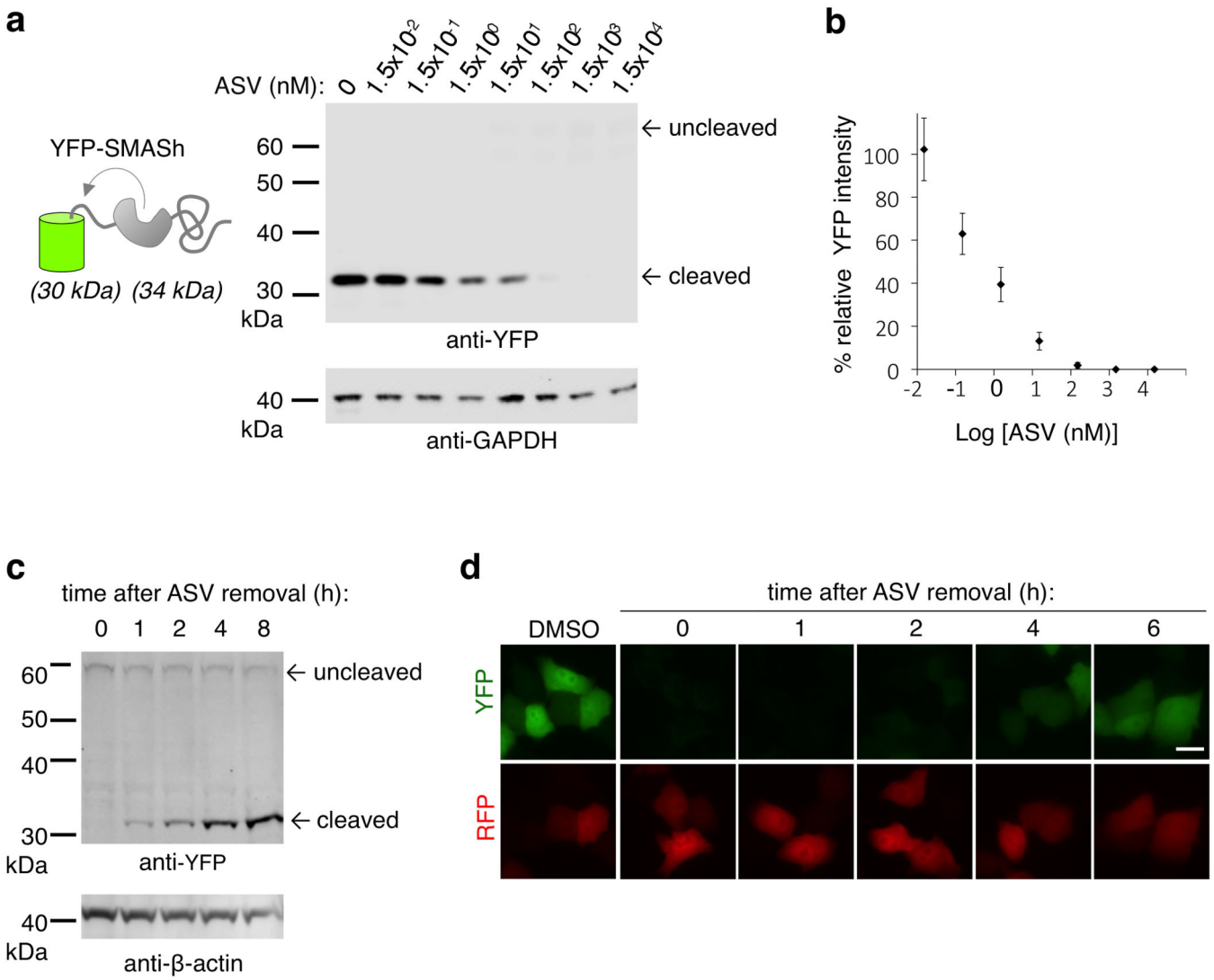

Figure 3.

Protein regulation by SMASh-tagging is dose-dependent and reversible. **(a)** To test dose-dependent regulation of protein expression by SMASh, HEK293 cells transfected with YFP-SMASh were cultured for 24 h without or with ASV (15 pM to 15 μM) and YFP was detected by immunoblot. GAPDH served as a loading control. **(b)** Quantification of YFP levels by immunoblot. Background-subtracted YFP signal was normalized to background-subtracted GAPDH signal, and then plotted as a percent of the signal in the untreated condition (n = 3, error bars represent standard deviations). **(c)** Restoration of YFP expression following drug washout, assayed by immunoblot. HeLa cells transfected with YFP-SMASh were grown 12 h in the presence of 2 μM ASV, then washed and exchanged into fresh media. Parallel wells were lysed at indicated times afterwards. β-actin served as a loading control. **(d)** Restoration of YFP expression following drug washout, assayed by fluorescence microscopy. HeLa cells co-transfected with untagged RFP and YFP-SMASh were grown 12 h in the presence of 2 μM ASV, washed, exchanged into fresh media, and imaged at

indicated times afterwards. Similarly transfected HeLa cells grown 12 h in DMSO are shown at left for comparison. Representative images are shown. Scale bar, 20 μm.

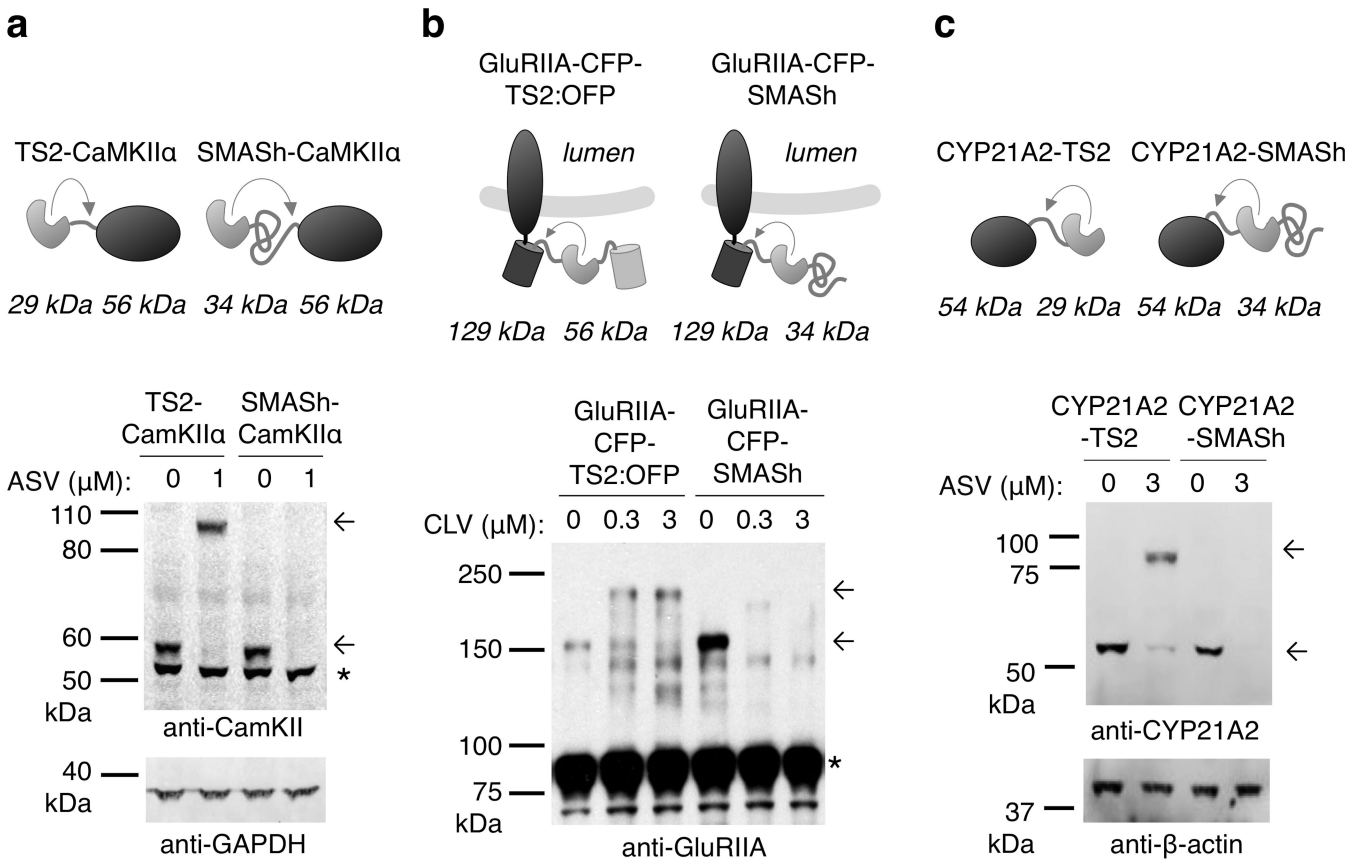

Figure 4.

SMASh functions on a variety of proteins. **(a)** SMASh functions on multimerizing protein, CaMKIIα. TimeSTAMP2-tagged CaMKIIα (TS2-CaMKIIα) or SMASh-CaMKIIα were expressed in HEK293 cells for 24 h in the absence or presence of ASV. The TimeSTAMP2 contain a cis-cleaving NS3 protease domain but lacks NS4A, verifying that drug inhibition of protein expression is specific to SMASh. Immunoblotting revealed shutoff of CaMKIIα expression by ASV when it was tagged with SMASh but not when it was tagged with TimeSTAMP2. GAPDH served as a loading control. The asterisk indicates a cross-reactive protein also detected in untransfected cells. The expected locations of the uncleaved higher molecular weight protein and the cleaved protein are indicated with arrows. **(b)** GluRIIA-CFP fused to TimeSTAMP2 with an orange fluorescent protein readout (GluRIIA-CFP-TS2:OFP) or GluRIIA-CFP-SMASh were expressed in HEK293 cells for 24 h in the absence or presence of ciluprevir (CLV). Immunoblotting revealed shutoff of GluRIIA expression by CLV. The non-degron-containing TS2:OFP tag verified that drug inhibition of protein expression is specific to SMASh. Cross-reactive bands at 80 kDa (asterisk) served as a lysate loading control. **(c)** CYP21A2 was either fused to TimeSTAMP2 or SMASh and tested with the same method as in (a). CYP21A2 level was detected by immunoblotting. β-actin served as a loading control.

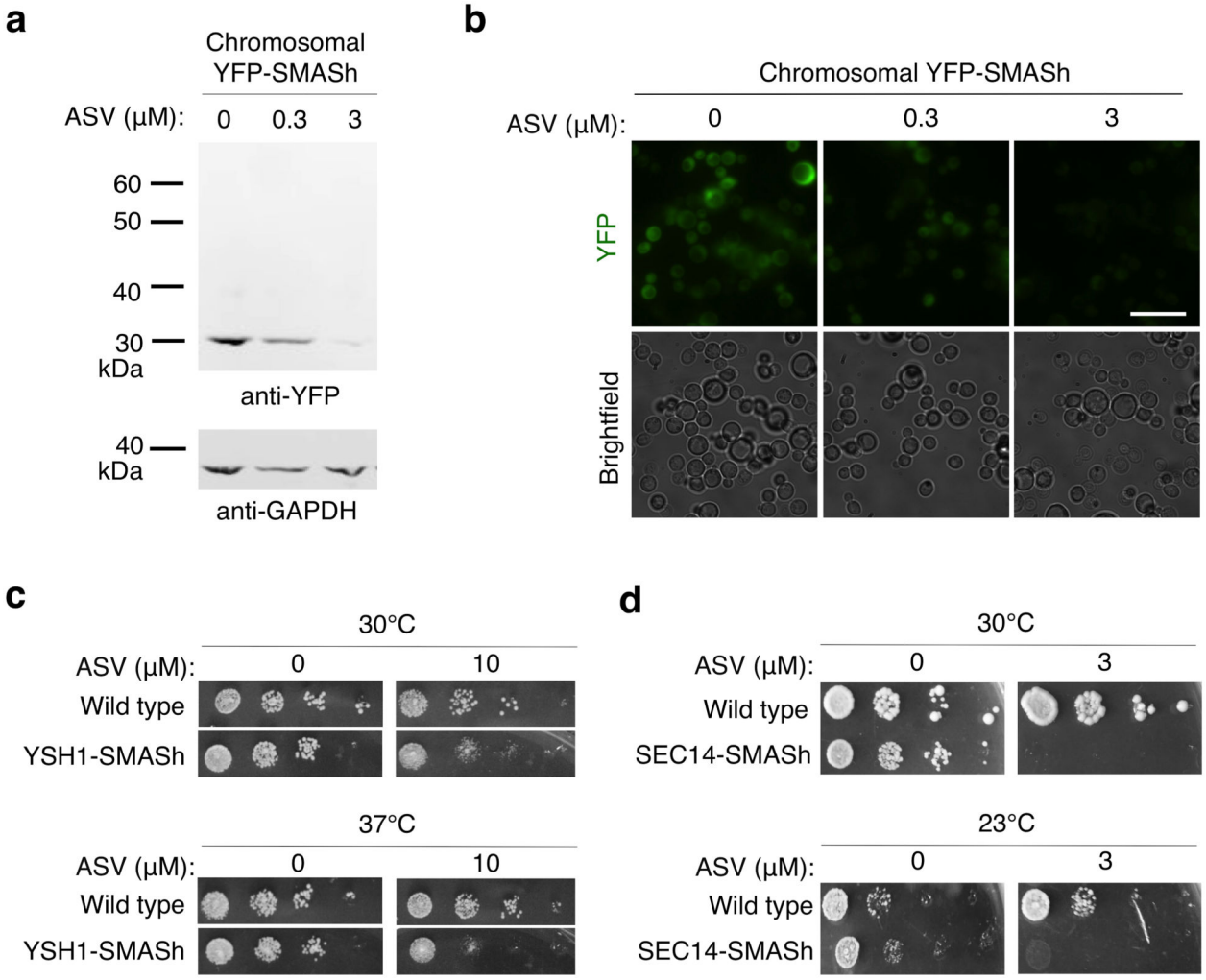

Figure 5.

SMASh functions in budding yeast. **(a)** YFP-SMASh under strong GPD promoter is integrated into the yeast chromosomal LUE locus. Recombinated yeast were cultured in SD media in the absence or presence of ASV for 24 h. Immunoblotting revealed shutoff of YFP expression by ASV. DMSO was used as vehicle control. GAPDH served as a loading control. **(b)** Fluorescence images of yeast cultures in (**a**) show that chromosomally-expressed YFP signal is controlled in a drug-dependent manner. Imaging was done in SD media. Scale bar, 10 μm. **(c)** An HA tag and the SMASh tag were inserted at the C-terminus of the endogenous SEC14 coding sequence, and serial dilutions of cells were plated and incubated for 48 h at 30 °C and 23 °C in the absence or presence of ASV (3 μM). **(d)** A SMASh tag was inserted at the C-terminus of the endogenous YSH1 coding sequence, and serial dilutions of cells were plated and incubated for 48 h at 30 °C and 37 °C in the absence or presence of ASV (10 μM).

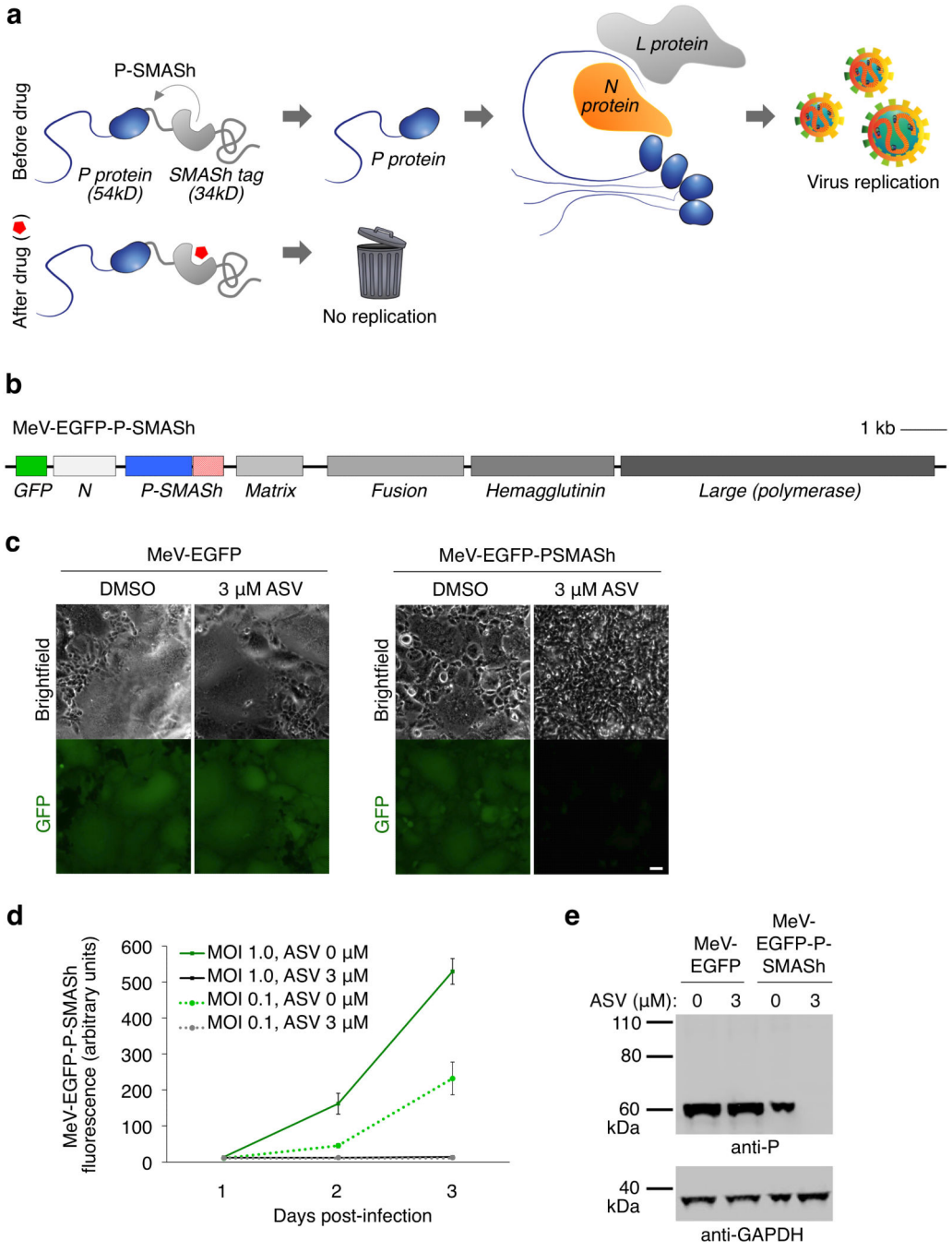

Figure 6.

Generation of a drug-controllable “SMAShable” measles vaccine virus. **(a)** Concept of controlling MeV replication with P-SMASh. In the absence of the drug, essentially unmodified phosphoprotein (P, blue) is released and can successfully form replication complexes with nucleocapsid (N, orange) and large (L) proteins. **(b)** Genome organization of MeV-EGFP-P-SMASh. Scale bar is 1 kilobase. **(c)** Regulation of MeV-EGFP-P-SMASh by drug. Vero cells infected with MeV-EGFP or MeV-EGFP-P-SMASh at multiplicity of infection (MOI) of 1 were grown for 72 h in the absence or presence of ASV. Drug inhibited

syncytium formation and GFP expression in MeV-EGFP-P-SMASh-infected but not MeV-EGFP-infected cells. Scale bar, 50 μm. **(d)** Quantification of fluorescence from Vero cells infected with MeV-EGFP-P-SMASh at MOI 1 and 0.1 in the absence or presence of 3 μM ASV (*n* = 3, error bars are standard deviation). **(e)** Drug inhibited P expression in MeV-EGFP-P-SMASh-infected but not MeV-EGFP-infected cells, as assayed by immunoblotting. GAPDH served as a loading control.